IEEE Access
Multidisciplinary | Rapid Review | Open Access Journal

Received March 27, 2022, accepted April 20, 2022, date of publication April 25, 2022, date of current version May 4, 2022.

Digital Object Identifier 10.1109/ACCESS.2022.3170145

Insulation Monitoring and Diagnosis of Faults in Cross-Bonded Cables Based on the Resistive Current and Sheath Current

BO ZHU, XIAOYANG YU, LIGANG TIAN, AND XINLAO WEI
School of Electrical and Electronic Engineering, Harbin University of Science and Technology, Harbin 150080, China

Corresponding author: Bo Zhu (zhubo1219@163.com)

This work was supported in part by the National Natural Science Foundation of China under Grant 51707048; and in part by the University Nursing Program for Young Scholars with Creative Talents in Heilongjiang Province, China, under Grant UNPYSCT-2018217.

ABSTRACT To reduce the induction voltage in the metal sheath, cross-bonded grounding is a widely adopted method in long-distance high voltage power cables, but this introduces challenges to the online monitoring and diagnosis of cable insulation. An online monitoring and diagnosis method for cable insulation based on the analysis of resistive current is proposed in this paper. A theoretical formula for the separation between leakage current and sheath current was derived, and a theoretical formula for the separation between resistive current and leakage current was obtained. An equivalent circuit of a three-phase long distance cable was established using the MATLAB/Simulink platform. The simulation was used to model three typical faults: cable insulation deterioration, open sheath circuit faults, and the sheath breakdown of intermediate joint faults. The results show that the method can be used to monitor each cable's insulation state under metal sheath cross-bonded, and it also can determine the open sheath circuit faults and fault joint location using the measured current values by the corresponding current sensors increases significantly. Based on the analyses, diagnostic criteria are established for different types of cable faults and fault locations.

INDEX TERMS Long distance power cable, cross-bonded, resistive current, leakage current, sheath current, fault diagnosis.

I. INTRODUCTION

In order to meet the demands for long-distance and large-capacity power delivery, high-voltage cables are widely used in power system transmission lines and in ultrahigh voltage transmission. A single-core structure is usually adopted for high-voltage cables. During operation, a high-value inductive voltage will be generated in the metal sheath. The value of the inductive voltage will increase with increasing cable length and will damage the outer sheath as well as the main insulation. Moreover, an unbalanced current in the metal sheath will limit the current-carrying capacity of the cable [1], [2]. To address the abovementioned problems, the cross interconnection of metal sheaths is adopted to reduce the circulation in the sheath and reduce the induced voltage [3], [4]. However, the cross-bonded connection design introduces new challenges to the online monitoring and diagnosis of cable insulation. At present, online monitoring methods for cable insulation status include dielectric loss monitoring, insulation resistance monitoring, and partial discharge monitoring [5]–[9]. These methods are mainly used for short-distance single-ended or double-ended grounding power cables. They are not applicable at 110 kV or above the voltage levels of cross-connected high-voltage cables; this limits the amount of research on the online monitoring of the insulation status of high-voltage cables under cross-connection [10]–[12].

Reference [13] proposed an insulation monitoring method for cross-connected cables using system power disturbance but ignored the fact that current sensors can be installed only on coaxial cables and that it is not possible to implement the installation of current sensors on every cross-connected line. Reference [14] proposed to monitor sheath-to ground current to detect cable sheath faults, but it cannot reflect the cable insulation condition. Reference [15] proposed a method of dielectric loss factor measurement to monitor the whole cable insulation condition, but it cannot detect partical cable faults under cross-bonded metal sheaths. Reference [16] established an equivalent circuit model for the sheath current of the

The associate editor coordinating the review of this manuscript and approving it for publication was Hui Ma.

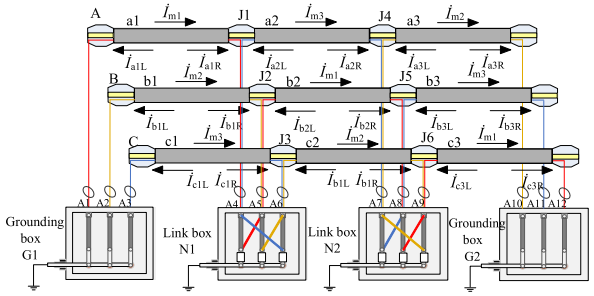

FIGURE 1. Schematic diagram of a unit of a cross-bonded three-phase cable.

cross-connected cable system and proposed an online monitoring and diagnosis method for high-voltage cable faults based on sheath current analysis, but the model ignored the influence of leakage current. The monitoring method proposed in [17] considers the influences of leakage current and sheath circulation but does not monitor the main insulation state of the cables. Reference [18] proposed an online method to monitor the relative change in dielectric loss between the phases of cross interconnections, but it gives a complex criterion for cable insulation aging, and the possible faults of the protective layer are ignored. Current research has not been realized to monitor each section of cable insulation after metal sheath interconnection.

The purpose of the paper is studying the way to solve the problem mentioned above. This paper presents a method for determining cable faults that uses the measured current on coaxial cables to calculate the resistive current flowing through the main insulation and the sheath circuit current. First, the resistive current and sheath current of the metal sheathed cross-bonded cable model under normal conditions are simulated and analyzed. Then, cable insulation faults and sheath circuit faults are simulated and analyzed. Finally, the simulation results and corresponding criteria for different cable faults are given.

II. METHOD

A. THREE-PHASE MODEL FOR A CROSS-BONDED CABLE

The long-distance three-phase cable is divided into several standard cross-bonded units, as shown in Fig. 1. Each phase cable in the cross-bonded unit is divided into three sections, and each section of the cable is connected by a coaxial cable through the link box and then grounded. When the load current flows through the cable core, an induced voltage will be generated in the metal sheath. Since both ends of each standard cross-bonded unit are grounded, the metal sheath forms a loop. In ideal cases, the sum of the induced voltages in the metal sheath of each branch is zero, and the circulation should also be zero. However, in the actual operation of the cable, the parameters for each segment of the cable are not identical. In addition, there is also asymmetric cable laying and an unbalanced load current that will lead to the induced voltages in the metal sheath of each branch not summing to zero. At this time, circulating current will appear in the sheath loop and flow along the direction of the sheath loop. During operation, the induced voltage in the metal sheath of each cable should not exceed 50 V [15], [19].

B. LEAKAGE CURRENT IN THE SHEATH

The leakage current flowing through the cable insulation includes resistive current and capacitive current. When the cable is in normal operation, the capacitive current is far greater than the resistive current. When the cable insulation deteriorates or becomes damaged, the capacitive current does not change, so it cannot reflect the insulation condition of the cable over time; however, the resistive current changes significantly at this time. Therefore, the change in resistive current can be used to assess the condition of the main cable insulation.

Current sensors A1-A12 are installed on the coaxial cable at the external outlet of grounding box G1, grounding box G2, link box N1 and link box N2. The measured currents are expressed as $\dot{I}_{\mathrm{A1}}-\dot{I}_{\mathrm{A2}}$, as shown in Fig. 1. The leakage current is the current flowing from the cable core through the main insulation to the metal sheath, and it can flow in the leftward or rightward directions in the metal sheath [17].

The expression is shown in (1),

$$\dot{I}_{ni} = \dot{I}_{ni\mathrm{L}} + \dot{I}_{ni\mathrm{R}} \tag{1}$$

In (1), $\dot{I}_{ni}$ is the leakage current of each section. $\dot{I}_{ni\mathrm{L}}$ is the current component to the left. $\dot{I}_{ni\mathrm{R}}$ is the rightward current component ($n = \mathrm{a}, \mathrm{b}, \mathrm{c}$, $i = 1, 2, 3$). The expressions for $\dot{I}_{\mathrm{A1}}-\dot{I}_{\mathrm{A12}}$ are as follows [18]:

$$\begin{cases}
\dot{I}_{\mathrm{A1}} = \dot{I}_{\mathrm{a1L}} + \dot{I}_{\mathrm{b2L}} + \dot{I}_{\mathrm{c3L}} - \dot{I}_{\mathrm{m1}} \\
\dot{I}_{\mathrm{A2}} = \dot{I}_{\mathrm{b1L}} + \dot{I}_{\mathrm{c2L}} + \dot{I}_{\mathrm{a3L}} - \dot{I}_{\mathrm{m2}} \\
\dot{I}_{\mathrm{A3}} = \dot{I}_{\mathrm{c1L}} + \dot{I}_{\mathrm{a2L}} + \dot{I}_{\mathrm{b3L}} - \dot{I}_{\mathrm{m3}} \\
\dot{I}_{\mathrm{A4}} = \left(-\dot{I}_{\mathrm{a1R}} + \dot{I}_{\mathrm{b2L}} + \dot{I}_{\mathrm{c3L}} - \dot{I}_{\mathrm{m1}}\right) \\
\qquad\quad - \left(-\dot{I}_{\mathrm{c1R}} + \dot{I}_{\mathrm{a2L}} + \dot{I}_{\mathrm{b3L}} - \dot{I}_{\mathrm{m3}}\right) \\
\dot{I}_{\mathrm{A5}} = \left(-\dot{I}_{\mathrm{b1R}} + \dot{I}_{\mathrm{c2L}} + \dot{I}_{\mathrm{a3L}} - \dot{I}_{\mathrm{m2}}\right) \\
\qquad\quad - \left(-\dot{I}_{\mathrm{a1R}} + \dot{I}_{\mathrm{b2L}} + \dot{I}_{\mathrm{c3L}} - \dot{I}_{\mathrm{m1}}\right) \\
\dot{I}_{\mathrm{A6}} = \left(-\dot{I}_{\mathrm{c1R}} + \dot{I}_{\mathrm{a2L}} + \dot{I}_{\mathrm{b3L}} - \dot{I}_{\mathrm{m3}}\right) \\
\qquad\quad - \left(-\dot{I}_{\mathrm{b1R}} + \dot{I}_{\mathrm{c2L}} + \dot{I}_{\mathrm{a3L}} - \dot{I}_{\mathrm{m2}}\right) \\
\dot{I}_{\mathrm{A7}} = \left(-\dot{I}_{\mathrm{c1R}} - \dot{I}_{\mathrm{a2R}} + \dot{I}_{\mathrm{b3L}} - \dot{I}_{\mathrm{m3}}\right) \\
\qquad\quad - \left(-\dot{I}_{\mathrm{b1R}} - \dot{I}_{\mathrm{c2R}} + \dot{I}_{\mathrm{a3L}} - \dot{I}_{\mathrm{m2}}\right) \\
\dot{I}_{\mathrm{A8}} = \left(-\dot{I}_{\mathrm{a1R}} - \dot{I}_{\mathrm{b2R}} + \dot{I}_{\mathrm{c3L}} - \dot{I}_{\mathrm{m1}}\right) \\
\qquad\quad - \left(-\dot{I}_{\mathrm{c1R}} - \dot{I}_{\mathrm{a2R}} + \dot{I}_{\mathrm{b3L}} - \dot{I}_{\mathrm{m3}}\right) \\
\dot{I}_{\mathrm{A9}} = \left(-\dot{I}_{\mathrm{b1R}} - \dot{I}_{\mathrm{c2R}} + \dot{I}_{\mathrm{a3L}} - \dot{I}_{\mathrm{m2}}\right) \\
\qquad\quad - \left(-\dot{I}_{\mathrm{a1R}} - \dot{I}_{\mathrm{b2R}} + \dot{I}_{\mathrm{c3L}} - \dot{I}_{\mathrm{m1}}\right) \\
\dot{I}_{\mathrm{A10}} = -\dot{I}_{\mathrm{a1R}} - \dot{I}_{\mathrm{b2R}} - \dot{I}_{\mathrm{c3R}} - \dot{I}_{\mathrm{m1}} \\
\dot{I}_{\mathrm{A11}} = -\dot{I}_{\mathrm{b1R}} - \dot{I}_{\mathrm{c2R}} - \dot{I}_{\mathrm{a3R}} - \dot{I}_{\mathrm{m2}} \\
\dot{I}_{\mathrm{A12}} = -\dot{I}_{\mathrm{c1R}} - \dot{I}_{\mathrm{a2R}} - \dot{I}_{\mathrm{b3R}} - \dot{I}_{\mathrm{m3}}
\end{cases} \tag{2}$$

The currents measured in the coaxial cables of link boxes N1 and N2 contain the current flowing through the metal sheaths of the two adjacent cables. $\dot{I}_{a\mathrm{L}}$, $\dot{I}_{b\mathrm{L}}$, and $\dot{I}_{c\mathrm{L}}$ ($i = 1, 2, 3$) are the leftward current components of each

cable. $\dot{I}_{ai\mathrm{R}}$, $\dot{I}_{bi\mathrm{R}}$, and $\dot{I}_{ci\mathrm{R}}$ $(i = 1, 2, 3)$ are the rightward current components of each cable. $\dot{I}_{\mathrm{m1}}$, $\dot{I}_{\mathrm{m2}}$, and $\dot{I}_{\mathrm{m3}}$ are the circulating currents in the sheaths of each branch. Using the expressions of current measured by the current sensors above, the following expressions for the leakage current of phases A and C can be deduced:

$$\begin{cases} \dot{I}_{\mathrm{a1}} - \dot{I}_{\mathrm{c1}} = \dot{I}_{\mathrm{A1}} - \dot{I}_{\mathrm{A3}} - \dot{I}_{\mathrm{A4}} \\ \dot{I}_{\mathrm{a2}} - \dot{I}_{\mathrm{c2}} = \dot{I}_{\mathrm{A6}} - \dot{I}_{\mathrm{A7}} \\ \dot{I}_{\mathrm{a3}} - \dot{I}_{\mathrm{c3}} = \dot{I}_{\mathrm{A9}} - \dot{I}_{\mathrm{A10}} + \dot{I}_{\mathrm{A12}} \end{cases} \tag{3}$$

After simplification, the formulae shown above lead to the expression

$$\begin{aligned} &\left(\dot{I}_{\mathrm{a1}} + \dot{I}_{\mathrm{a2}} + \dot{I}_{\mathrm{a3}}\right) - \left(\dot{I}_{\mathrm{c1}} + \dot{I}_{\mathrm{c2}} + \dot{I}_{\mathrm{c3}}\right) = \dot{I}_{\mathrm{A1}} \\ &\quad -\dot{I}_{\mathrm{A3}} - \dot{I}_{\mathrm{A4}} + \dot{I}_{\mathrm{A6}} - \dot{I}_{\mathrm{A7}} + \dot{I}_{\mathrm{A9}} - \dot{I}_{\mathrm{A10}} + \dot{I}_{\mathrm{A12}} \end{aligned} \tag{4}$$

At the same time, the following expressions for the leakage current of cables in phases A and B can be obtained:

$$\begin{cases} \dot{I}_{\mathrm{b1}} - \dot{I}_{\mathrm{a1}} = \dot{I}_{\mathrm{A2}} - \dot{I}_{\mathrm{A5}} - \dot{I}_{\mathrm{A1}} \\ \dot{I}_{\mathrm{b2}} - \dot{I}_{\mathrm{a2}} = \dot{I}_{\mathrm{A4}} - \dot{I}_{\mathrm{A8}} \\ \dot{I}_{\mathrm{b3}} - \dot{I}_{\mathrm{a3}} = \dot{I}_{\mathrm{A7}} - \dot{I}_{\mathrm{A11}} + \dot{I}_{\mathrm{A10}} \end{cases} \tag{5}$$

After simplification, the following formula can be obtained:

$$\begin{aligned} &\left(\dot{I}_{\mathrm{b1}} + \dot{I}_{\mathrm{b2}} + \dot{I}_{\mathrm{b3}}\right) - \left(\dot{I}_{\mathrm{a1}} + \dot{I}_{\mathrm{a2}} + \dot{I}_{\mathrm{a3}}\right) = -\dot{I}_{\mathrm{A1}} \\ &\quad +\dot{I}_{\mathrm{A2}} + \dot{I}_{\mathrm{A4}} - \dot{I}_{\mathrm{A5}} + \dot{I}_{\mathrm{A7}} - \dot{I}_{\mathrm{A8}} + \dot{I}_{\mathrm{A10}} - \dot{I}_{\mathrm{A11}} \end{aligned} \tag{6}$$

The relationship between the sum of the currents in the three loop circuits and the current measured by the current sensor is

$$\begin{cases} \dot{I}_{\mathrm{a1}} + \dot{I}_{\mathrm{b2}} + \dot{I}_{\mathrm{c3}} = \dot{I}_{\mathrm{A1}} - \dot{I}_{\mathrm{A10}} \\ \dot{I}_{\mathrm{b1}} + \dot{I}_{\mathrm{c2}} + \dot{I}_{\mathrm{a3}} = \dot{I}_{\mathrm{A2}} - \dot{I}_{\mathrm{A11}} \\ \dot{I}_{\mathrm{c1}} + \dot{I}_{\mathrm{a2}} + \dot{I}_{\mathrm{b3}} = \dot{I}_{\mathrm{A3}} - \dot{I}_{\mathrm{A12}} \end{cases} \tag{7}$$

After simplification, the following can be obtained:

$$\begin{aligned} &\left(\dot{I}_{\mathrm{a1}} + \dot{I}_{\mathrm{a2}} + \dot{I}_{\mathrm{a3}}\right) + \left(\dot{I}_{\mathrm{b1}} + \dot{I}_{\mathrm{b2}} + \dot{I}_{\mathrm{b3}}\right) + \left(\dot{I}_{\mathrm{c1}} + \dot{I}_{\mathrm{c2}} + \dot{I}_{\mathrm{c3}}\right) \\ &\quad = \left(\dot{I}_{\mathrm{A1}} - \dot{I}_{\mathrm{A12}}\right) + \left(\dot{I}_{\mathrm{A2}} - \dot{I}_{\mathrm{A10}}\right) + \left(\dot{I}_{\mathrm{A3}} - \dot{I}_{\mathrm{A11}}\right) \end{aligned} \tag{8}$$

We replace (4) and (6) with (8) to obtain

$$\begin{cases} \dot{I}_{\mathrm{a1}} + \dot{I}_{\mathrm{a2}} + \dot{I}_{\mathrm{a3}} = \dfrac{1}{3} \\ \times\left(3\dot{I}_{\mathrm{A1}} - 3\dot{I}_{\mathrm{A10}} - 2\dot{I}_{\mathrm{A4}} - 2\dot{I}_{\mathrm{A7}} + \dot{I}_{\mathrm{A5}} + \dot{I}_{\mathrm{A6}} + \dot{I}_{\mathrm{A8}} + \dot{I}_{\mathrm{A9}}\right) \\ \dot{I}_{\mathrm{b1}} + \dot{I}_{\mathrm{b2}} + \dot{I}_{\mathrm{b3}} = \dfrac{1}{3} \\ \times\left(3\dot{I}_{\mathrm{A2}} - 3\dot{I}_{\mathrm{A11}} - 2\dot{I}_{\mathrm{A5}} - 2\dot{I}_{\mathrm{A8}} + \dot{I}_{\mathrm{A4}} + \dot{I}_{\mathrm{A6}} + \dot{I}_{\mathrm{A7}} + \dot{I}_{\mathrm{A9}}\right) \\ \dot{I}_{\mathrm{c1}} + \dot{I}_{\mathrm{c2}} + \dot{I}_{\mathrm{c3}} = \dfrac{1}{3} \\ \times\left(3\dot{I}_{\mathrm{A3}} - 3\dot{I}_{\mathrm{A12}} - 2\dot{I}_{\mathrm{A6}} - 2\dot{I}_{\mathrm{A9}} + \dot{I}_{\mathrm{A4}} + \dot{I}_{\mathrm{A5}} + \dot{I}_{\mathrm{A7}} + \dot{I}_{\mathrm{A8}}\right) \end{cases} \tag{9}$$

In (9), $\dot{I}_{ai}$, $\dot{I}_{bi}$, and $\dot{I}_{ci}$ $(i = 1, 2, 3)$ are the leakage current of each section in the A-, B-, and C-phase cables. Therefore, the leakage current can be separated from the circulating current of the cable sheath using (9).

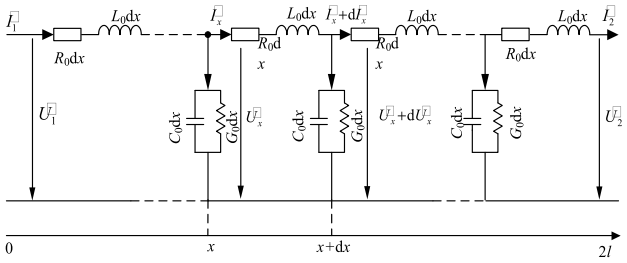

FIGURE 2. The equivalent of single phase power cable under AC steady condition.

C. RESISTIVE CURRENT SEPARATION

The Fig. 2 is the equivalent circuit of single phase cable under AC steady condition. Assumes the length of cable is $2l$, x is the any point of the cable, take a differential section dx, the current of x point is $\dot{I}_x$ and the current of $x + dx$ point is $\dot{I}_x + d\dot{I}_x$, the voltage of x point is $\dot{U}_x$ and the voltage of $x+dx$ point is $\dot{U}_x + d\dot{U}_x$, $\dot{U}_1$ and $\dot{U}_2$ are the voltage at both ends of cable, $\dot{I}_1$ and $\dot{I}_2$ are the current at both ends of cable core, R_0 and L_0 are the equivalent resistance and inductance per unit length of cable core, G_0 and C_0 are the equivalent conductance and capacitance per unit length of cable insulation [15]. When the voltage and current at head of cable are known, the voltage of x point is [20]:

$$\dot{U}_x = \dot{U}_1 \cosh(\gamma x) - Z_c \dot{I}_1 \sinh(\gamma x) \tag{10}$$

where Z_c is wave impedance, γ is propagation coefficient, which can be expressed as:

$$\begin{cases} \gamma = \sqrt{Z_0 Y_0} = \sqrt{(G_0 + \mathrm{j}\omega C_0)(R_0 + \mathrm{j}\omega L_0)} \\ Z_c = \sqrt{\dfrac{Z_0}{Y_0}} = \sqrt{\dfrac{R_0 + \mathrm{j}\omega L_0}{G_0 + \mathrm{j}\omega C_0}} \end{cases} \tag{11}$$

Similarly, when the current and voltage at end of cable are known, the voltage of x point is [20]:

$$\dot{U}_x = \dot{U}_2 \cosh\left[\gamma\,(l - x)\right] + Z_c \dot{I}_2 \sinh\left[\gamma\,(l - x)\right] \tag{12}$$

When x is equal $2l$, the difference between head and end of cable can be expressed as (13):

$$\begin{aligned} \dot{U}_1 - \dot{U}_2 &= \left[\dot{U}_2 \cosh(2\gamma l) + Z_c \dot{I}_2 \sinh(2\gamma l)\right] - \dot{U}_2 \\ &= -2\dot{U}_2 \sinh^2(\gamma l) + Z_c \dot{I}_2 \sinh(2\gamma l) \end{aligned} \tag{13}$$

When x is equal zero, the difference between head and end of cable can be expressed as (14):

$$\begin{aligned} \dot{U}_1 - \dot{U}_2 &= \dot{U}_1 - \left[\dot{U}_1 \cosh(2\gamma l) + Z_c \dot{I}_1 \sinh(2\gamma l)\right] \\ &= 2\dot{U}_1 \sinh^2(\gamma l) + Z_c \dot{I}_1 \sinh(2\gamma l) \end{aligned} \tag{14}$$

Combine (13) and (14), it can be obtained:

$$\frac{\left(\dot{U}_1 + \dot{U}_2\right)/2}{\dot{I}_1 - \dot{I}_2} = \frac{Z_c \sinh(2\gamma l)}{-4\sinh^2(\gamma l)} = Z \tag{15}$$

According to the circuit impedance theorem, (15) is the equivalent impedance Z of cable insulation, which is the ratio of half of the voltage phasor sum and the current difference

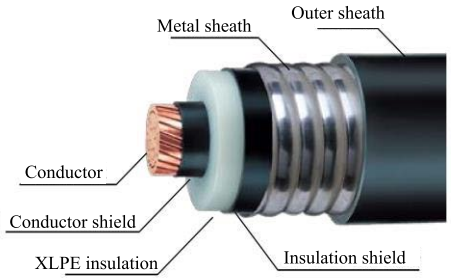

FIGURE 3. The structure of 110kV XLPE cable.

at both ends of the cable [15]. According to the definition of impedance, the equivalent resistance R and equivalent impedance C are:

$$Z = \frac{1}{1/R + \mathrm{j}\omega C} \tag{16}$$

where, ω is the angular velocity. Combine (15) and (16), R can be expressed as:

$$R = \frac{1}{\mathrm{Re}\left(\dot{I}/\dot{U}\right)} = \frac{1}{\mathrm{Re}\left(\frac{\dot{I}_1 - \dot{I}_2}{(\dot{U}_1 + \dot{U}_2)/2}\right)} \tag{17}$$

The resistive current and capacitive current can be obtained:

$$\dot{I}_R = \frac{\dot{U}}{R} = \frac{(\dot{U}_1 + \dot{U}_2)}{2} \cdot \mathrm{Re}\left(\frac{\dot{I}_1 - \dot{I}_2}{(\dot{U}_1 + \dot{U}_2)/2}\right) \tag{18}$$

The leakage current is the difference between head and end current of cable core, which can be obtained the leakage current of three phases cable are:

$$\begin{cases} \dot{I}_{A1} - \dot{I}_{A2} = \dot{I}_{a1} + \dot{I}_{a2} + \dot{I}_{a3} \\ \dot{I}_{B1} - \dot{I}_{B2} = \dot{I}_{b1} + \dot{I}_{b2} + \dot{I}_{b3} \\ \dot{I}_{C1} - \dot{I}_{C2} = \dot{I}_{c1} + \dot{I}_{c2} + \dot{I}_{c3} \end{cases} \tag{19}$$

TABLE 1. Parameters of 110 kV XLPE cable.

Parameter	Value
Cross-sectional conductors (mm^2)	800
Cable external diameter (mm)	100
Conductor diameter (mm)	34
Insulation thickness (mm)	16
Conductor shield (mm)	1.2
Insulation shield (mm)	1.0
Metal sheath (mm)	2.0
Sheath thickness (mm)	4.5

where $\dot{I}_{Ai}$, $\dot{I}_{Bi}$, and $\dot{I}_{Ci}$ $(i = 1, 2)$ are the current at both ends of cable core. Take (9) and (19) into (18), the total resistive currents flowing through the A-, B- and C-phase cable insulations are (20), as shown at the bottom of the next page, where $\dot{U}_{ai}$, $\dot{U}_{bi}$, and $\dot{U}_{ci}$ $(i = 1, 2)$ are the voltage at both ends of three-phase cable, $\dot{I}_{air}$, $\dot{I}_{bir}$, and $\dot{I}_{cir}$ $(i = 1, 2, 3)$ are the resistive current of each section in the A-, B-, and C-phase cables. Therefore, the calculation formula of resistive current can be used (20).

III. ETABLISHMENT AND VERIFICATION OF A THREE-PHASE CABLE SIMULATION

A 110 kV XLPE power cable is chosen as the focus for this study, the structure of cable is shown in Fig. 3 and the structural parameters of the cable are shown in Table 1.

According to the structural parameters of 110 kV XLPE cable in Table 1, the primary parameters of the cable can be calculated as follows: R_0 is $3.281 \times 10^{-5}\Omega$/m, L_0 is 2.139×10^{-7} H/m, G_0 is 1.396×10^{-11} S/m, C_0 is 1.972×10^{-10} F/m. The MATLAB/Simulink dynamic simulation platform was used to establish a three-phase cable simulation model, as shown in Fig. 4.

In the Fig. 4, U_a U_b U_c are the three-phase voltage source, U1-U6 are the voltage measurement module, A1-A6 are the current measurement module, load is RLC type load. To make the whole simulation model simply, put every two

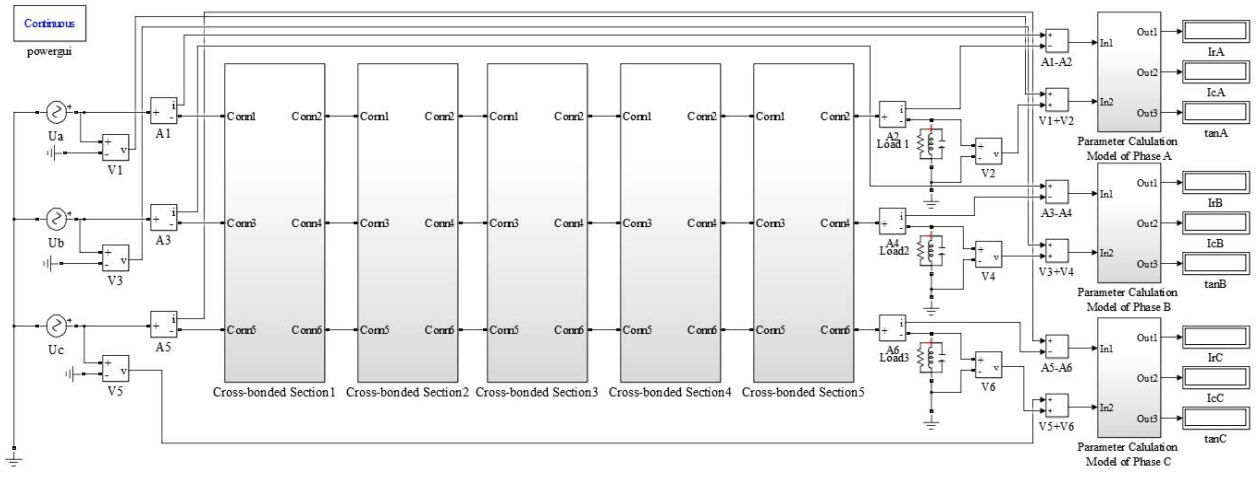

FIGURE 4. Simulation circuit of three phase long distance power cable under metal sheath cross-bonded.

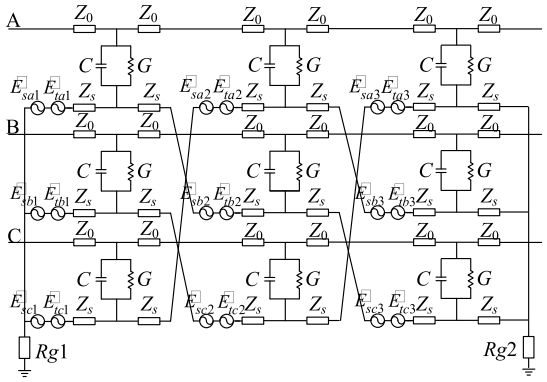

FIGURE 5. Equivalent circuit of a unit of a cross-bonded three-phase cable.

metal sheath cross-bonded units into cross-bonded sections and put (20) into the calculation module to calculate the effective value. The results are displayed by display module. The Fourier module is used in calculate module to extract the fundamental component of voltage and current which make the calculation process is not effected by harmonic. The whole cable length is 12000 m, which has five cross-bonded sections in cable model. A cross-bonded unit is taken as an example for analysis. The equivalent circuit of a unit of a cross-bonded cable is shown in Fig. 5.

In Fig. 5, $\dot{E}_{\mathrm{sa}i}$, $\dot{E}_{\mathrm{sb}i}$, and $\dot{E}_{\mathrm{sc}i}$ $(i = 1, 2, 3)$ are the induced voltages caused by A-, B-, and C-phase cable cores in section i, respectively. $\dot{E}_{\mathrm{ta}i}$, $\dot{E}_{\mathrm{tb}i}$, and $\dot{E}_{\mathrm{tc}i}$ $(i = 1, 2, 3)$ are the induced voltages in the A-, B-, and C-phase cables caused by the current in the metal sheath of other phases and the ground circulation, respectively. Z_0 is the equivalent impedance of the cable core. Z_s is the equivalent impedance of the metal sheath. R_{g1} and R_{g2} are the grounding resistances at the two ends of the cable's metal sheath.

To facilitate calculation, it is assumed that the leakage current flows out from the midpoint of the metal sheath in each section. The cross-bonded unit cable length is 1200 m, and the length of each section is 400 m after the cable is divided into three sections. The parameters for each section of the cable are identical. The system voltage is 110 kV, and the grid frequency is 50 Hz. The resistive currents of the a1-a2-a3, b1-b2-b3, and c1-c2-c3 branches and the currents of the a1-b2-c3, b1-c2-a3, c1-a2-b3 loops are simulated. The branch current simulation results are shown in Table 2.

TABLE 2. The theoretical and simulation value of I_r.

Parameter	Theoretical values (mA)	Simulation values (mA)	Relative error (%)
a1-a2-a3	1.842	1.843	0.05
b1-b2-b3	1.842	1.843	0.05
c1-c2-c3	1.842	1.843	0.05
a1-b2-c3	1.986	1.988	0.1
b1-c2-a3	1.986	1.988	0.1
c1-a2-b3	1.986	1.988	0.1
a1-a2-a3	1.842	1.843	0.05

The theoretical values of each branch current are calculated the sum of the resistive current flowing through the each section of cable insulation. The simulation values are calculated by using (20). The theoretical values are essentially consistent with the simulation values, validating the accuracy and feasibility of this method.

IV. FAULT DETECTION AND ANALYSIS

A study on cable insulation fault and sheath circuit fault is conducted. Cable insulation faults are primarily described by the decrease in cable insulation resistance caused by cable aging and moisture. The faults in the sheath circuit arise either from the sheath circuit becoming an open circuit or from the electrical breakdown of the intermediate joint sheath resulting in a short circuit. In this paper, the common cable faults are divided into three categories, namely, cable insulation deterioration, open circuit fault in the protective layer circuit, and the breakdown of the protective layer of the intermediate joint.

A. CABLE INSULATION FAULT

The main causes for cable insulation fault include moisture, deterioration, external damage, and manufacturing defects. Long-distance power cables are composed of multiple cross-interconnected units in series. Each cross-bonded unit contains nine cables. The online monitoring of cable insulation can be realized by calculating the resistive current in each phase of the cable and the loop current in the sheath of each cross-interconnected unit and by observing the change in the relationship between them. In the simulation model, the normal value of each cable insulation equivalent resistance is 179 MΩ. Set the equivalent resistance 25 MΩ of A-phase

$$\begin{cases} \dot{I}_{a1r} + \dot{I}_{a2r} + \dot{I}_{a3r} = \dfrac{(\dot{U}_{a1} + \dot{U}_{a2})}{2} \cdot \mathrm{Re}\left(\dfrac{\frac{1}{3}\left(3\dot{I}_{\mathrm{A}1} - 3\dot{I}_{\mathrm{A}10} - 2\dot{I}_{\mathrm{A}4} - 2\dot{I}_{\mathrm{A}7} + \dot{I}_{\mathrm{A}5} + \dot{I}_{\mathrm{A}6} + \dot{I}_{\mathrm{A}8} + \dot{I}_{\mathrm{A}9}\right)}{(\dot{U}_{a1} + \dot{U}_{a2})/2} \right) \\ \dot{I}_{b1r} + \dot{I}_{b2r} + \dot{I}_{b3r} = \dfrac{(\dot{U}_{b1} + \dot{U}_{b2})}{2} \cdot \mathrm{Re}\left(\dfrac{\frac{1}{3}\left(3\dot{I}_{\mathrm{A}2} - 3\dot{I}_{\mathrm{A}11} - 2\dot{I}_{\mathrm{A}5} - 2\dot{I}_{\mathrm{A}8} + \dot{I}_{\mathrm{A}4} + \dot{I}_{\mathrm{A}6} + \dot{I}_{\mathrm{A}7} + \dot{I}_{\mathrm{A}9}\right)}{(\dot{U}_{b1} + \dot{U}_{b2})/2} \right) \\ \dot{I}_{c1r} + \dot{I}_{c2r} + \dot{I}_{c3r} = \dfrac{(\dot{U}_{c1} + \dot{U}_{c2})}{2} \cdot \mathrm{Re}\left(\dfrac{\frac{1}{3}\left(3\dot{I}_{\mathrm{A}3} - 3\dot{I}_{\mathrm{A}12} - 2\dot{I}_{\mathrm{A}6} - 2\dot{I}_{\mathrm{A}9} + \dot{I}_{\mathrm{A}4} + \dot{I}_{\mathrm{A}5} + \dot{I}_{\mathrm{A}7} + \dot{I}_{\mathrm{A}8}\right)}{(\dot{U}_{c1} + \dot{U}_{c2})/2} \right) \end{cases} \tag{20}$$

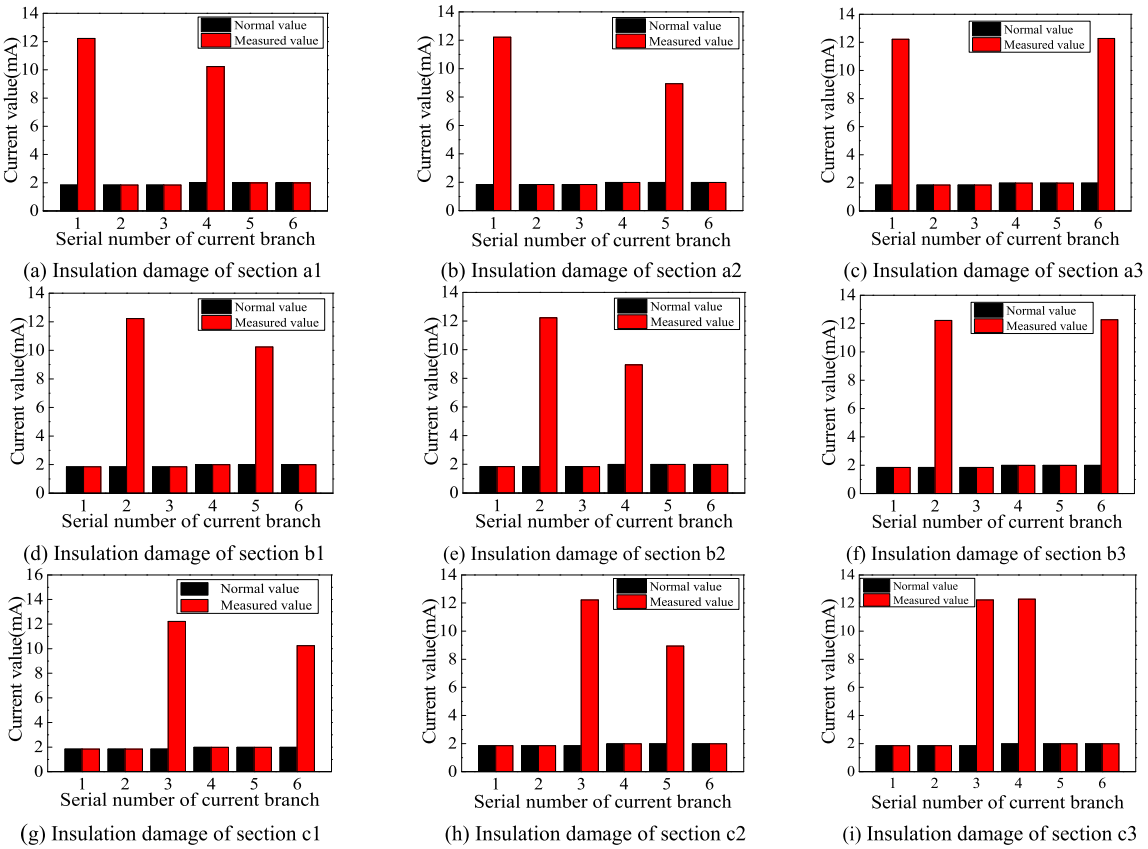

FIGURE 6. Insulation fault in each cable section.

TABLE 3. The diagnostic criteria of insulation faults.

Fringing of current	a1-a2-a3	b1-b2-b3	c1-c2-c3
a1-b2-c3	a1	b2	c3
b1-c2-a3	a3	b1	c2
c1-a2-b3	a2	b3	c1

section a_1 to characterize the insulation fault. Similarly, set the equivalent resistance of other eight cables. The relationship between the insulation fault of each cable and the current branch is shown in Fig. 6.

The abscissa numbers from 1 to 6 in Fig. 6 denote the a1-a2-a3, b1-b2-b3, c1-c2-c3, a1-b2-c3, b1-c2-a3 and c1-a2-b3 current branches. The simulation results show that when the resistive current in branch a1-a2-a3 increases, an insulation fault occurs in the A-phase cable. If the current in the a1-b2-c3 loop increases, the insulation fault can be located in section a1. The insulation condition of other cables can be determined using the same method, and the diagnostic criteria are shown in Table 3. The diagnostic criteria of method can diagnose each cable's insulation state under metal sheath cross-bonded.

B. OPEN CIRCUIT FAULT OF THE METAL SHEATH

The main reasons for open circuit fault in the protective layer include improper installation, external force damage to the protective layer, and loose connections between the coaxial cable and the metal protective layer due to the corrosion of the connection parts. This study considers the sheath open circuit faults in the cable grounding box, link box, intermediate joint, and their influences.

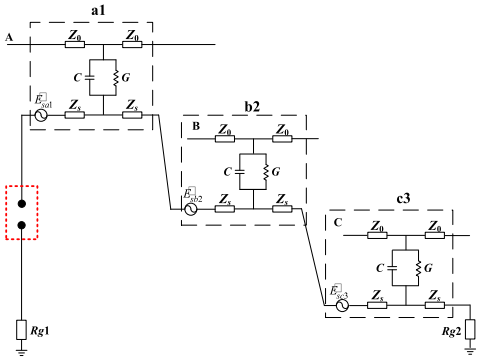

FIGURE 7. Equivalent circuit of open circuit in G1.

1) OPEN-CIRCUIT FAULTS IN THE GROUNDING BOXES OF G1 AND G2

When an open circuit fault occurs in the grounding boxes of G1 and G2, any branch of a1-b2-c3, b1-c2-a3, and c1-a2-b3 can become an open circuit. At this time, there is no circulating current in the branch, and there is a leakage

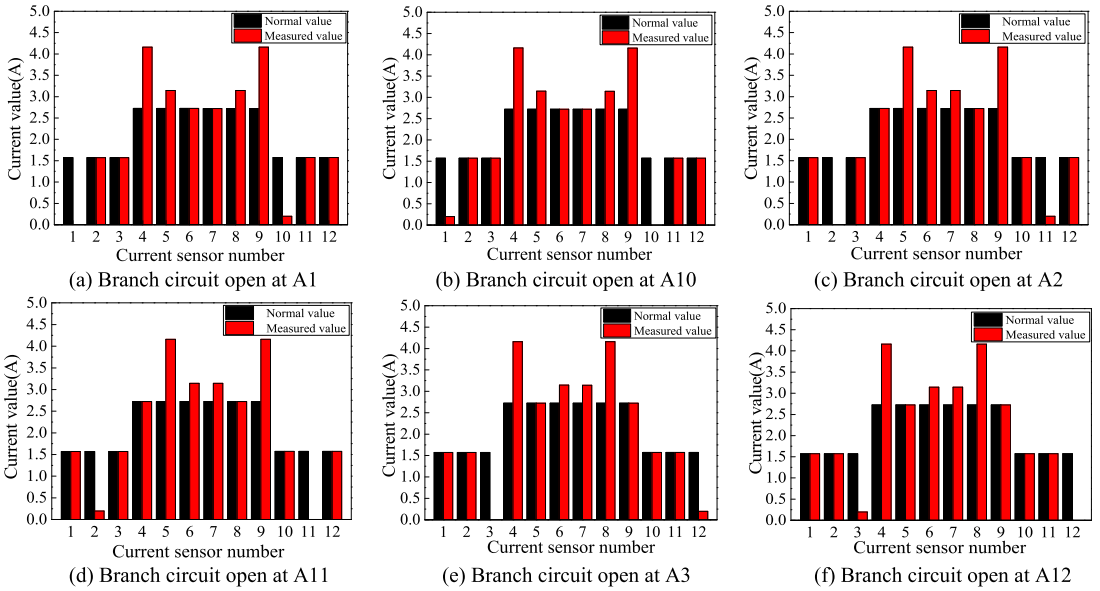

FIGURE 8. Open circuit fault in the grounding box.

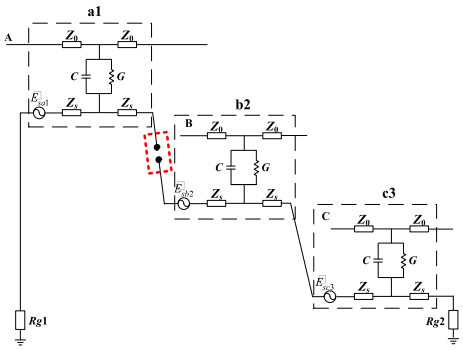

FIGURE 9. Equivalent circuit of open circuit in N1.

TABLE 4. The diagnostic criteria of open circuit faults in link box.

Grounding Box	Open Circuit Position	Measured Current (mA)	
G1	A1	A1=0	A10=1.988
	A2	A2=0	A11=1.988
	A3	A3=0	A12=1.988
G2	A10	A1=1.988	A10=0
	A11	A2=1.988	A11=0
	A12	A3=1.988	A12=0

current only from the main insulation of the cable to the protective layer. The simulation results show that the current values of the a1-b2-c3, b1-c2-a3, and c1-a2-b3 loops and the resistive current values of the a1-a2-a3, b1-b2-b3, and c1-c2-c3 branches do not change. At this time, the position of the open-circuit fault can be determined only by the measured current value at each current sensor. Fig. 7 is the equivalent circuit of open circuit in the grounding boxes of G1.

The simulation results are shown in Fig. 8. The serial numbers 1-12 of the abscissa in the figure represent the

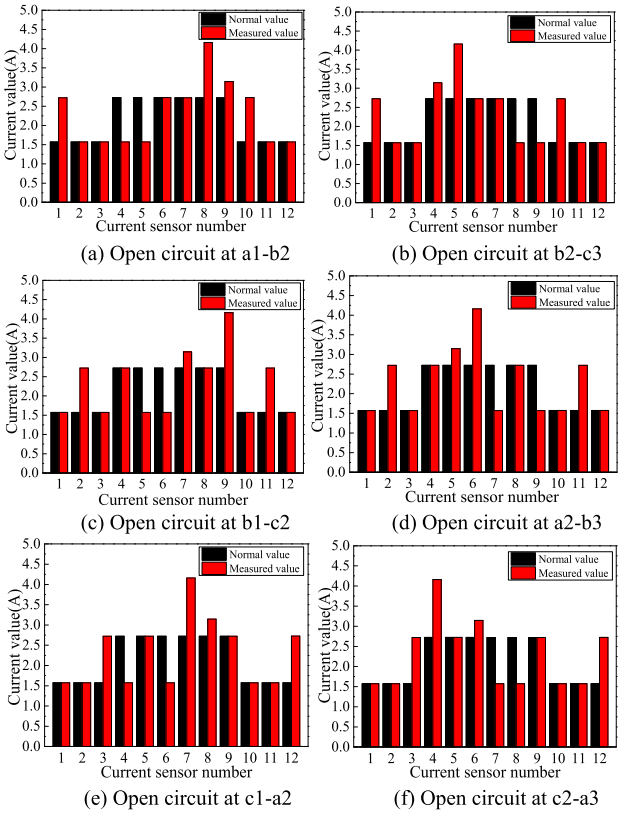

FIGURE 10. Open circuit fault in the link box.

current measured by current sensors A1-A12, respectively. The simulation results show that the location of the open circuit fault in the protective layer in the grounding box is related to the measured value at each current sensor. The diagnostic criterion for the open circuit fault of the protective layer in the grounding box is shown in TABLE 4.

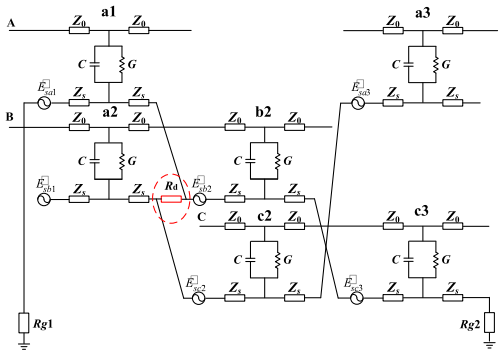

FIGURE 11. Equivalent circuit of short-circuit fault due to the breakdown point between b1 and b2 metal sheath in joint J2.

Therefore, the specific location of the open circuit fault can be determined using the measured current values from current sensors A1, A2, and A3 in grounding box G1 and current sensors A10, A11, and A12 in grounding box G2.

2) OPEN CIRCUIT FAULT IN LINK BOXES

The coaxial cables in link boxes N1 and N2 are connected to two branches. When the sheath open-circuit fault occurs, the current values of the a1-b2-c3, b1-c2-a3, and c1-a2-b3 loops and the resistive current values of the a1-a2-a3, b1-b2-b3, and c1-c2-c3 branches do not change. At this time, the open-circuit position can be determined only by the variational patterns of the measured current of the current sensors A1–A12. Fig. 9 is the equivalent circuit of open circuit in link boxes N1.

The simulation results of the open circuit fault of the protective layer at different locations and the current measured by each current sensor are shown in Fig. 10. Fig. 10(a), (c) and (e) are simulation results from the model with an open circuit fault in link box N1, and Fig. 10(b), (d) and (f) are simulation results from the model with an open circuit fault in link box N2. According to the results of Fig. 10(a) and (b), when the open circuit fault occurs in the a1-b2 or b2-c3 section of the a1-b2-c3 branch, the currents measured by the current sensors A1 and A10 will increase. According to Fig. 10(a), the currents measured by A8 and A9 increase, and the measured currents measured by A4 and A5 decrease. This is because the open circuit fault in the a1-b2 section leads to the measured current flowing through A4 and A5 changing from the original two branch currents to a single branch current and results in the decrease of the measured current flowing through A4 and A5; the measured current flowing through A8 and A9 changes from the original state of flowing both leftward and rightward to a current component that flows only rightward, resulting in an increase in the measured current; this is evidence that the open circuit fault occurs in link box N1. It can be seen from Fig. 10(b) that the current measured by sensors A4 and A5 increases, while the current measured by A8 and A9 decreases. It can be concluded that the open circuit fault is located in link box N2. Similarly, according to the variation of the current measured by each current sensor in Fig. 10(c), (d) and (e), (f), it can be concluded that the open circuit fault occurs in link boxes N1 or N2. The diagnostic criteria of open circuit fault in the link box are shown in Table 5.

TABLE 5. The diagnostic criteria of open circuit faults in link box.

Link box	Open Circuit	Sensors with increasing current (A)			
N1	a1-b2	A1=2.7	A8=4.2	A9=3.1	A10=2.7
	b1-c2	A2=2.7	A7=3.1	A9=4.2	A11=2.7
	c1-a2	A3=2.7	A7=4.2	A8=3.1	A12=2.7
N2	a2-b3	A3=2.7	A4=4.2	A6=3.1	A12=2.7
	b2-c3	A1=2.7	A4=3.1	A5=4.2	A10=2.7
	c2-a3	A2=2.7	A5=3.1	A6=4.2	A11=2.7

TABLE 6. The diagnostic criteria of joints breakdown.

Fault Joint	Fault section	Sensors with increasing current (A)			
J1	a1-a2	A1=14.5	A3=14.5	A6=14.5	A8=14.5
J2	a2-a3	A1=14.5	A2=14.5	A4=14.5	A9=14.5
J3	b1-b2	A2=14.5	A3=14.5	A5=14.5	A7=14.5
J4	b2-b3	A6=14.5	A8=14.5	A11=14.5	A12=14.5
J5	c1-c2	A4=14.5	A9=14.5	A10=14.5	A12=14.5
J6	c2-c3	A5=14.5	A7=14.5	A10=14.5	A11=14.5

C. BREAKDOWN FAULT AT THE INTERMEDIATE JOINT

When the intermediate joint of the cable is improperly installed or the quality of materials is below standard, it is easy for the protective layer in the intermediate joint to break

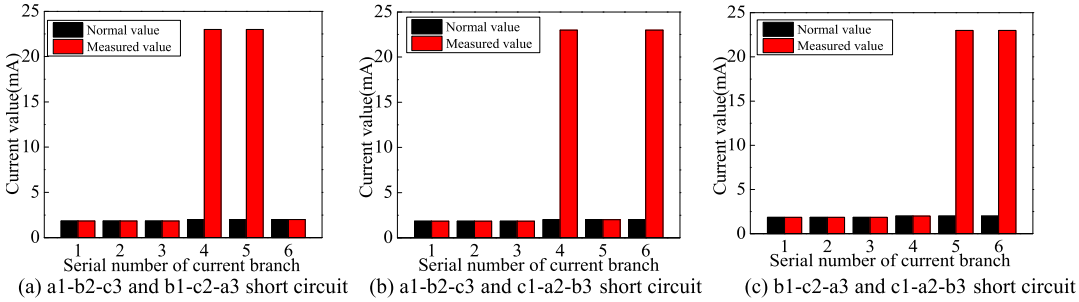

FIGURE 12. Breakdown fault at the intermediate joint of the cable.

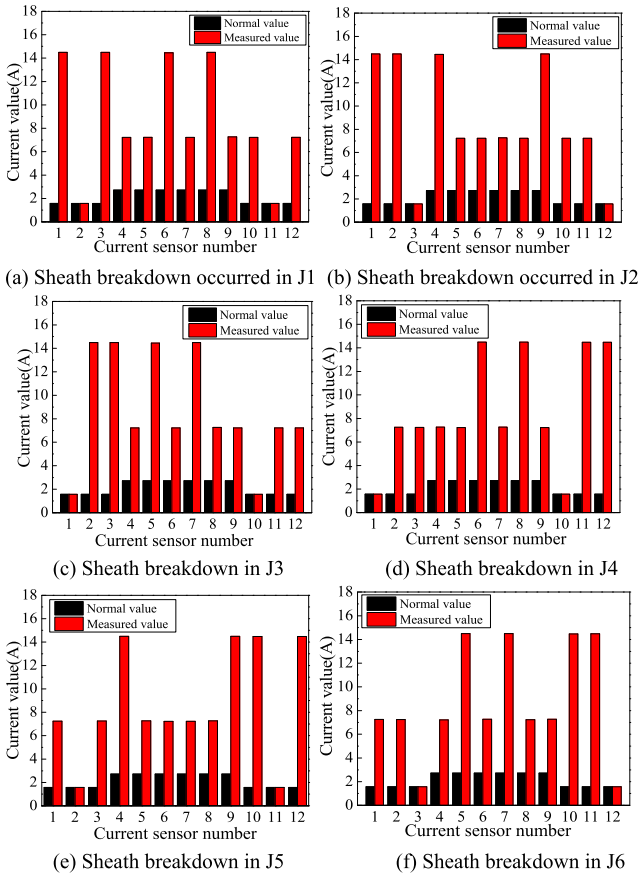

FIGURE 13. **Measured current of each current sensor when the cable intermediate joint breaks down.**

down and result in a new current channel between the two protective layers. In cable joint J1–J6, as shown in Fig. 1, the breakdown of the J1 or J5 internal sheath will cause branches a1-b2-c3 and c1-a2-b3 to short circuit; the breakdown of the J2 or J6 internal sheath will cause branches a1-b2-c3 and b1-c2-a3 to short circuit, and the breakdown of the J3 or J4 internal sheath will cause branches b1-c2-a3 and c1-a2-b3 to short circuit. The equivalent circuit of the breakdown fault in joint J2 is shown in Fig. 11.

The simulation results are shown in Fig. 12. In Fig. 12, it can be seen that the branch current of the short circuit increases. The measured currents of the three branches a1-a2-a3, b1-b2-b3, and c1-c2-c3 are unchanged. This can be used to determine which branch is short circuited, but this cannot determine which intermediate joint internal protection layer has experienced breakdown. Therefore, it is necessary to determine the position of the fault joint according to the change in the current measured by sensors A1–A12. The simulation results are shown in Fig. 13.

It can be seen from Fig. 13 that when the protective layer breakdown occurs inside the joint, the current in the two branches connected to the joint will significantly increase, and the current measured by the current sensors in these two branches will also further increase. The joint breakdown diagnostic criteria are shown in Table 6.

In Table 6, when protective layer breakdown occurs in the J1 joint, the measured current from sensors A1, A3, A6 and A8 will increase more significantly. When the protective layer breakdown occurs in joint J2, the current measured by current sensors A1, A2, A4 and A9 increases more significantly. Similarly, when the protective layer breakdown occurs in the other four joints, the current measured by the corresponding current sensors increases more significantly. Therefore, we can determine which joint breaks down using the simulation results.

V. CONCLUSION

In this paper, a procedure for using resistive current and sheath current for assessing the insulation state of cables is proposed. An equivalent model of cross-bonded cables is established, and a simulation study is carried out. Finally, the following conclusions are obtained:

(1) Through the analysis of the current in the protective layer, the leakage current and resistive current are separated, and a calculation for the resistive current is performed. The simulation study verifies the accuracy of this method. The method makes on-line insulation monitoring and diagnosis of faults in cross-bonded cables possible.

(2) To study insulation faults of the cable, the diagnosis of each cable's insulation state in each cross-bonded unit is performed. The results show that the diagnostic criteria can be used to monitor each cable's insulation state under metal sheath cross-bonded.

(3) For the open-circuit faults of metal sheath, the specific location can be determined using the measured current values from current sensors which are installed on coaxial cables at grounding boxes or link boxes. The diagnostic criterion for the open circuit fault is proposed.

(4) For the breakdown fault at the intermediate joint, the location of fault joint can be determined using the measured current values by the corresponding current sensors increases significantly. The diagnostic criteria of joint breakdown are summarized.

REFERENCES

[1] U. Stella Gudmundsdottir, B. Gustavsen, C. Leth Bak, and W. Wiechowski, "Field test and simulation of a 400-kV cross-bonded cable system," *IEEE Trans. Power Del.*, vol. 26, no. 3, pp. 1403–1410, Jul. 2011.

[2] E. Riva Sanseverino, V. Li Vigni, A. Di Stefano, and R. Candela, "A two-end traveling wave fault location system for MV cables," *IEEE Trans. Ind. Appl.*, vol. 55, no. 2, pp. 1180–1188, Apr. 2019.

[3] Z. Li, B. Du, and W. Li, "Evaluation of high-voltage AC cable grounding systems based on the real-time monitoring and theoretical calculation of grounding currents," *High Voltage*, vol. 3, no. 1, pp. 38–43, Mar. 2018.

[4] S. M. Gargari, P. A. A. F. Wouters, P. C. J. M. van der Wielen, and E. F. Steennis, "Partial discharge parameters to evaluate the insulation condition of on-line located defects in medium voltage cable networks," *IEEE Trans. Dielectr. Electr. Insul.*, vol. 18, no. 3, pp. 868–877, Jun. 2011.

[5] M. Li, C. Zhou, and W. Zhou, "A novel fault location method for a cross-bonded HV cable system based on sheath current monitoring," *Sensors*, vol. 18, no. 10, p. 3356, Oct. 2018.

[6] M. Li, C. Zhou, and W. Zhou, "Feasibility study on lengthening the high-voltage cable section and reducing the number of cable joints via alternative bonding methods," *High Voltage*, vol. 4, no. 4, pp. 292–299, Dec. 2019.

[7] G. S. Zhang, J. Y. Liu, S. M. Zhang, G. Taylor, and Y. B. Liu, "An investigation of frequency fluctuation impact on isolated power system self-excitation," in *Proc. Asia–Pacific Power an Energy Eng. Conf.*, Wuhan, China, Mar. 2011, pp. 1–5.
[8] R. Bartnikas, "Partial discharges. Their mechanism, detection and measurement," *IEEE Trans. Dielectr. Electr. Insul.*, vol. 9, no. 5, pp. 763–808, Oct. 2002.
[9] F. D. Leon, M. L. Marquez-Asensio, and G. Alvarez-Cordero, "Effects of conductor counter-transposition on the positive-sequence impedance and losses of cross-bonded cables," *IEEE Trans. Power Del.*, vol. 26, no. 3, pp. 2060–2063, Jul. 2011.
[10] I. Lafaia, J. Mahseredjian, A. Ametani, T. C. Barros, I. Kocar, and Y. Fillion, "Frequency and time domain responses of cross-bonded cables," in *Proc. IEEE Power Energy Soc. Gen. Meeting (PESGM)*, Portland, OR, USA, Aug. 2018, pp. 640–648.
[11] B. Sheng, W. Zhou, J. Yu, S. Meng, C. Zhou, and D. M. Hepburn, "On-line PD detection and localization in cross-bonded HV cable systems," *IEEE Trans. Dielectr. Insul.*, vol. 21, no. 5, pp. 2217–2224, Oct. 2014.
[12] O. M. K. K. Nanayakkara, A. D. Rajapakse, and R. Wachal, "Traveling-wave-based line fault location in star-connected multiterminal HVDC systems," *IEEE Trans. Power Del.*, vol. 27, no. 4, pp. 2286–2294, Oct. 2012.
[13] J. Barros, M. Apraiz, and R. I. Diego, "Review of signal processing techniques for detection of transient disturbances in voltage supply systems," in *Proc. IEEE Int. Instrum. Meas. Technol. Conf. (I2MTC)*, Minneapolis, MN, USA, May 2013, pp. 450–455.
[14] M. Marzinotto and G. Mazzanti, "The feasibility of cable metal sheath fault detection by monitoring metal sheath-to-ground currents at the ends of cross-bonding sections," *IEEE Trans. Ind. Appl.*, vol. 51, no. 6, pp. 5376–5384, Nov./Dec. 2015.
[15] B. Pang, B. Zhu, X. Wei, S. Wang, and R. Li, "On-line monitoring method for long distance power cable insulation," *IEEE Trans. Dielectrics Electr. Insul.*, vol. 23, no. 1, pp. 70–76, Feb. 2016.
[16] M. Adel Shokry, A. Khamlichi, F. Garnacho, J. Martínez Malo, and F. Álvarez, "Detection and localization of defects in cable sheath of cross-bonding configuration by sheath currents," *IEEE Trans. Power Del.*, vol. 34, no. 4, pp. 1401–1411, Aug. 2019.
[17] X. Dong, Y. Yang, C. Zhou, and D. M. Hepburn, "Online monitoring and diagnosis of HV cable faults by sheath system currents," *IEEE Trans. Power Del.*, vol. 32, no. 5, pp. 2281–2290, Oct. 2017.
[18] Y. Yang, D. M. Hepburn, C. Zhou, W. Zhou, and Y. Bao, "On-line monitoring of relative dielectric losses in cross-bonded cables using sheath currents," *IEEE Trans. Dielectr. Electr. Insul.*, vol. 24, no. 5, pp. 2677–2685, Oct. 2017.
[19] F. P. Ebrahimi and M. G. Ahsaee, "Accurate and comprehensive fault location algorithm for two-terminal transmission lines," *IET Gener., Transmiss. Distrib.*, vol. 12, no. 19, pp. 4334–4340, Oct., 2018.
[20] B. Zhu, L. Tian, X. Wei, and H. Nie, "Calculation method of equivalent core impedance and admittance parameters of long distance power cable," in *Proc. IEEE Int. Conf. High Voltage Eng. Appl. (ICHVE)*, Sep. 2020, pp. 1–4.

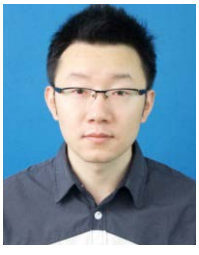

BO ZHU received the B.Sc., M.Sc., and Ph.D. degrees in high voltage and insulation technology from the Harbin University of Science and Technology, China, in 2010, 2013, and 2015, respectively. He is currently an Associate Professor with the School of Electrical and Electronic Engineering, Harbin University of Science and Technology. His research interests include online monitoring of cable insulation and high voltage test.

XIAOYANG YU received the B.S. degree in electromagnetic measurement technology and instruments from the Harbin Institute of Electrical Engineering, Harbin, China, in 1984, and the M.S. and Ph.D. degrees in precision instruments and machinery from the Harbin Institute of Technology, Harbin, in 1989 and 1998, respectively. Since 1999, he has been a Professor with the Harbin University of Science and Technology. His research interests include three-dimensional visual inspection, tissue optical characteristic imaging, and image processing.

LIGANG TIAN was born in Liaoning, China, in 1995. He received the B.Sc. degree from Liaoning Petrochemical University, Fushun, China, in 2018, and the master's degree from the Harbin University of Science and Technology, Harbin, China, in 2021. His research interest includes online monitoring of cable insulation.

XINLAO WEI received the B.Sc. degree in high voltage technology and equipment from Xi'an Jiaotong University, China, in 1982, the M.Sc. degree in high voltage technology from the Beijing Electric Power Research Institute, China, in 1988, and the Ph.D. degree in electrical machine from the Harbin Institute of Technology, China, in 2003. From 1982 to 1995, he was with the Harbin Institute of Electrical Engineering. He is currently a Professor at the Harbin University of Science and Technology. His major research interests include high voltage insulation and online monitoring of electric equipment.